DESCRIPTION AND VALIDATION OF THE ONERA COMPUTATIONAL METHOD FOR THE PREDICTION OF BLADE-VORTEX INTERACTION NOISE

P. Beaumier, Applied Aerodynamics Department, ONERA, Châtillon, France

Y. Delrieux, Department of Numeric Simulation and Acoustics, ONERA, Châtillon, France

Abstract

The computational method used at ONERA for the prediction of Blade-Vortex Interaction (BVI) noise is presented in this paper. The five steps of the computational chain are first described. The calculations are then validated by comparison with two different databases. The first one was obtained in the HART program; in this case, it is shown that the influence of Higher Harmonic Control (HHC) on wake geometry and radiated noise is well captured. The second one was obtained in the ERATO program, where a passive blade shape optimisation was done: in this case, the calculations succeed in predicting the relative difference in noise levels between the ERATO optimised blade compared to a reference blade, although the wake geometry of the ERATO rotor is not well captured. Finally, strategies to reduce the BVI noise for blades equipped with trailing-edge flaps are proposed.

Introduction

It is well known that the major reason for limiting the use of helicopters in urban areas is the amount of noise radiated by this aircraft. More precisely, among the various noise sources, the so-called Blade Vortex Interaction noise (BVI) is the most penalising for the helicopter in approaching flight (low speed descent or fly-over conditions). This is the reason why many efforts have been devoted all over the world during the last twenty years to develop, validate and apply numerical methods aiming at predicting the BVI noise in view of its reduction.

The objective of the present paper is to illustrate the current status of the methodology used at ONERA to compute the BVI noise. Particular emphasis is laid on the prediction of the wake developed by the main rotor, which is the key parameter for an accurate acoustic prediction.

In a first part, a description of each of the five components of the ONERA computational chain is done and the reasons for this decomposition of the calculations are explained.

The computational chain is then validated by comparison with two different databases. The first one is the HART database, obtained in 1994 in the framework of a multinational research cooperation (between NASA, US Army, the DLR, the DNW and ONERA). This HART database is very well suited for code validation since it includes information about aerodynamics (blade pressure, vortex positions, field velocities), dynamics (elastic deformations) and acoustics, on the Bo105 model rotor. The second one is the ERATO database, obtained in 1998 in the framework of the bilateral French-German cooperation between ONERA, DLR and Eurocopter. Here, the computational chain was used to optimise the blade geometry in order to reduce the BVI noise.

The last part of the paper is devoted to the prediction of BVI noise for a more advanced and recent program (the ABC French-German program, dealing with Active Blade Concept), for which no experimental database is presently available for validation. Specific adaptations of the computational method to compute blades with trailing-edge flaps are described and typical results of calculations are presented. In order to find optimal flap deflections to reduce the BVI noise, different mechanisms of noise reduction are investigated.

Computational Method

The computational method used at ONERA for the prediction of the BVI noise generated by helicopter rotors had been set-up progressively between 1990 and 1995. Since that time, different adaptations of this method have been done but the general philosophy has remained unchanged. First of all, it has to be well understood that the radiated BVI noise is a consequence of several interactions between the vortices (generally tip vortices, but not always) emitted by the blades and the following blades; these interactions generate pressure fluctuations on the blades that are the source of the so-called BVI noise. So, the first step of the computational method is to compute accurately the unsteady pressure fluctuations encountered by the blades during their rotation. Simple considerations allow to understand that this phenomenon is very impulsive: as an example, for conditions typical of strong BVI noise, the time necessary for the vortex to travel from the blade leading-edge to the blade trailing-edge is of the order of 3° of azimuth (for interactions on the advancing side of the rotor disk). This means that it is essential to be able to compute the positions and strengths of the vortices (and more generally of the wake generated by the blades) with a very fine time discretisation. Since CFD methods (Euler or Navier-Stokes methods) were not (and even today are not) accurate enough to convect vortices over large distances, it was preferred to rely on singularity methods, and more precisely on methods that are able to compute distorted wakes (and vortex) geometry. However, it is well known that such methods become very time consuming when the time (and space) discretisation is reduced. In order to avoid too large CPU time, it has been decided to develop at ONERA a computation chain which computes separately the wake characteristics and the resulting blade pressure fluctuations.

In fact, the computational method is made of five main steps: the rotor trim, the wake prediction, the roll-up model, the calculation of blade pressure and finally the noise radiation. Each of these steps is described hereafter.

Rotor trim (HOST or R85 code)

Given the flight conditions that have to be simulated (advancing speed, rotor thrust, flapping piloting law…), the first step of the computational chain is to determine the blades rigid and aero-elastic dynamic response. Up to 1996, this was done by the R85 code [1] developed by Eurocopter for isolated rotor simulations. A more general tool (the HOST code [2]), applicable not only for isolated rotor but also for a complete helicopter, has been developed since that time by Eurocopter. The numerical models used in R85 and HOST codes are very similar. Both codes solve the Lagrange equations for each degree of freedom (d.o.f.), representing the equilibrium of the system composed by the rotor blades:

$$\frac{d}{dt}\frac{\partial T}{\partial \dot{q}_i} - \frac{\partial T}{\partial q_i} + \frac{\partial U_{el}}{\partial q_i} = Q_i$$

with:

- T=kinetic energy calculated using the general structure mechanics relations,
- U_{el}=elastic energy, written as a function of the elastic d.o.f.,
- Q_i=generalized forces of external loads (aerodynamic).

The aerodynamic model in based on the lifting-line theory, for which the sectional lift (Cl), drag (Cd) and pitching moment (Cm) coefficients are directly interpolated into 2D airfoil tables depending on the local sectional Mach number and incidence. A singularity method simulates the inflow through the rotor disk: a wake of prescribed helical geometry (Figure 1, left) is used, made of vortex lattices the circulation of which is deduced from the spanwise and azimuthal variations of the blade circulation. An iterative coupling between the circulation on the blades and the velocities induced by the wake on the rotor disk (calculated using the Biot&Savart law) is done inside the trim loop.

The elastic model is based on a simple beam model with 3 d.o.f. (chordwise and flapwise bending, torsion). In order to reduce the number of unknowns, each d.o.f. is projected on a modal basis (rotor eigenmodes). For periodic simulations (which is the case for all the conditions presented here), each d.o.f. is decomposed into Fourier series.

Wake prediction (MESIR code)

As a result of the preceding step, the rigid and aero-elastic blade motion is known. However the prescribed wake model used during the trim procedure in R85 or HOST codes is not sufficient for an accurate prediction of blade-vortex interactions. A second step is necessary to iteratively distort the initial wake geometry under its own aerodynamic influence. This is made by the MESIR code [3] which computes (using the Biot&Savart law) the velocities induced by all vortex lattices at each discretisation point of the wake and modifies accordingly the wake geometry. An inner loop between the circulation on the blades and the velocities induced on the rotor disk is necessary for each new wake geometry. The wake is then iteratively distorted (outer loop) until convergence, which is achieved when the position of vortex lattices between two consecutive modifications of the wake geometry remains unchanged. Figure 1 (right) provides an example of a distorted wake geometry.

Note that the blade motion remains unchanged during this second step of the computational chain. In other terms, this means that it is assumed that the distorted wake geometry has no significant influence on the rotor trim: such an assumption will be discussed in the paper.

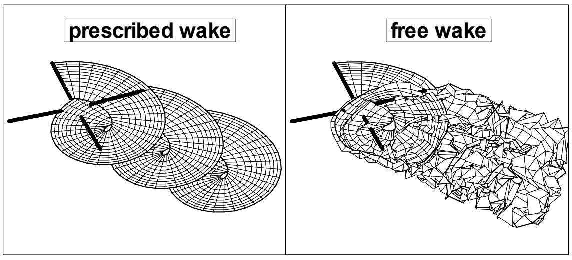

Figure 1: Wake generated by one blade. Prescribed helical geometry (left) and distorted geometry (right).

Roll-up Model (MENTHE code)

An intermediate step between wake and pressure calculations is introduced in the computational method. It consists in modelling the roll-up of the vortices, and is performed by the MENTHE code [4]. MENTHE identifies the portions of the MESIR predicted vortex sheets the intensity of which is sufficient to result in a roll-up. The intensities and radial locations of the rolled-up vortices, which constitute the interacting vortices, are determined at the emission azimuths.

Blade pressure (ARHIS code)

Blade pressure distribution is then calculated by the unsteady singularity method ARHIS [5]. This code assumes that the flow around the rotor is inviscid and incompressible. It performs 2D-by-slices calculations. Subsonic compressibility effects are included by means of Prandtl-Glauert corrections combined with local thickening of the airfoil. In addition, finite span effects are introduced through an elliptic-type correction of the pressure coefficients. The interacting vortices are modelled as freely convecting and deforming clouds of vortex elements. The main advantage of this method is its ability to take into account the vortex deformation during strong blade-vortex interactions. A variable azimuthal step, depending on the impulsiveness of the interaction is used.

Noise radiation (PARIS code)

The noise radiation is computed by the PARIS code [6], starting from the pressure distribution provided by ARHIS. PARIS is based on the Ffowcs Williams-Hawkings equations and predicts the loading and thickness noise. It uses a time domain formulation. An efficient spanwise interpolation method has been implemented [7], which identifies the BVI impulsive events on the signatures generated by each individual blade section.

Validation on HART database

The results presented in this part are related to the HART I project (called HART hereafter), carried out before year 1995 [9]. No results related to the more recent HART II project are presented.

The multinational project HART had the objective to gain a physical understanding of the mechanisms involved in BVI. To achieve this, a hingeless Bo105 model rotor was tested in the DNW 6x8m open test section in June 1994 [8], leading to a very complete database including aerodynamic, dynamic and acoustic results, together with information about some parts of the rotor wake by Laser Doppler Velocimetry (LDV) and Laser Light Sheet (LLS) techniques. The rotor main characteristics are:

- 4 blades,
- radius R=2m, chord length c=0.121m,
- rectangular planform with modified NACA23012 airfoil,
- linear aerodynamic twist -8°/R.

Test cases

Among the large number of test conditions tested in the DNW, three of them are selected for the present validation: they are all defined by a rotating velocity Ω=1040rpm, an advancing speed V_0=33m/s (advance ratio μ=0.15), a rotor thrust coefficient Ct≈0.0044, a rotor shaft angle α_s=5.3°, and are typical of descent flight configurations for which significant BVI noise occurs. The three cases are:

- the Baseline case (BA), with a conventional monocyclic pitch command,
- the Minimum Noise case (MN), with a 3/rev multicyclic pitch command of amplitude A_3≈0.8°, and for which the phase has been adjusted to minimise the radiated noise,
- the Minimum Vibration (MV) case, with a 3/rev multicyclic pitch command of the same amplitude A_3, but with a different phase adjusted to minimise the vibrations.

The objective of this part is not to analyse and explain the influence of HHC on the blade-vortex interactions (for this, the reader should refer to [9], [10]), but to check how each step of the computational chain compares with experimental data.

Validation of the rotor trim

In the calculations, the rotor trim is done to match the experimental values of V_0, Ct and α_s=5.3° and to ensure 0 hub moments, which is the way the rotor trim was done during the tests. The resulting commands of the rotor (collective and cyclic pitch angles) are compared with experimental values in Figure 2. Whatever the test case is (BA, MN or MV), the collective pitch angle is overestimated by the calculations by about 1.9°, which is quite large (Figure 2, left): it will be seen below that this is a consequence of an underestimation of the mean value of the elastic torsion deformation, which is compensated by a larger collective pitch to ensure the correct rotor thrust coefficient Ct. The longitudinal cyclic pitch angle θ_{1C} is systematically slightly underestimated by the predictions by about 0.5° (Figure 2, middle): this could be due to the influence of the model support, which often modifies the longitudinal trim of the rotor. The lateral cyclic pitch angle θ_{1S} is relatively well predicted, with differences with experiment which are less than 0.4° (Figure 2, right).

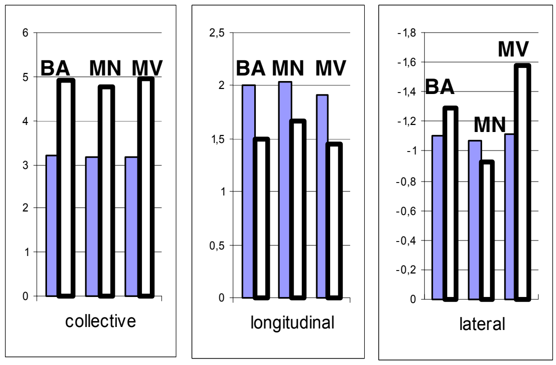

Figure 2: Experimental (full bars) and predicted (hollow bars) pitch angles.

Airloads prediction: low frequency

It is very important to check that the sectional airloads azimuthal histories calculated just after the trim and wake analysis are consistent with experimental data. Considering the large azimuthal step used in the wake prediction code MESIR, only the low frequency components of the airloads are relevant for comparison. Such a comparison is done on the CnM2 coefficients, derived from the experiment by integration of the pressure data measured by the unsteady pressure transducers. As an example, the CnM2 azimuthal histories, filtered below the 8th rotational frequency, are plotted in Figure 3 for the spanwise location r/R=0.87. Generally speaking, the calculations are in good agreement with experiment. For the Baseline case, the 1/rev and 2/rev oscillations of the airloads are fairly well predicted (Figure 3, top), even if the amplitude of the 2/rev component is underestimated. For the two other cases (MN and MV), the CnM2 azimuthal histories are dominated by a 3/rev component, as a consequence of the 3/rev HHC excitation: the amplitude and phase of this 3/rev component are well predicted, although the 3/rev amplitude is slightly underestimated. Note that the area of negative loading for the MV case (Figure 3, bottom) and the area of large positive loading for the MN case (Figure 3, middle) in the second quadrant (around ψ=130°) are well captured by MESIR calculations, which is very important since it is the area where the vortices known to be responsible for noise are emitted. In fact, most of the features of the low frequency airloads can be understood by comparing the torsion blade tip response (Figure 4). It is clear that the mean value of the elastic deformations are underestimated by the calculations (by about 2°), which gives an explanation for the overestimation of the collective pitch angles, as noticed in the previous paragraph. In addition it can be seen that the 2/rev component of the torsion in the Baseline case is not captured by the calculations, which explains the underestimation of the 2/rev components of the airloads. Similarly, the 3/rev component of the torsion of the MN and MV cases is captured with the correct phase but with a too low amplitude, which explains why a similar trend is observed on the CnM2 coefficients.

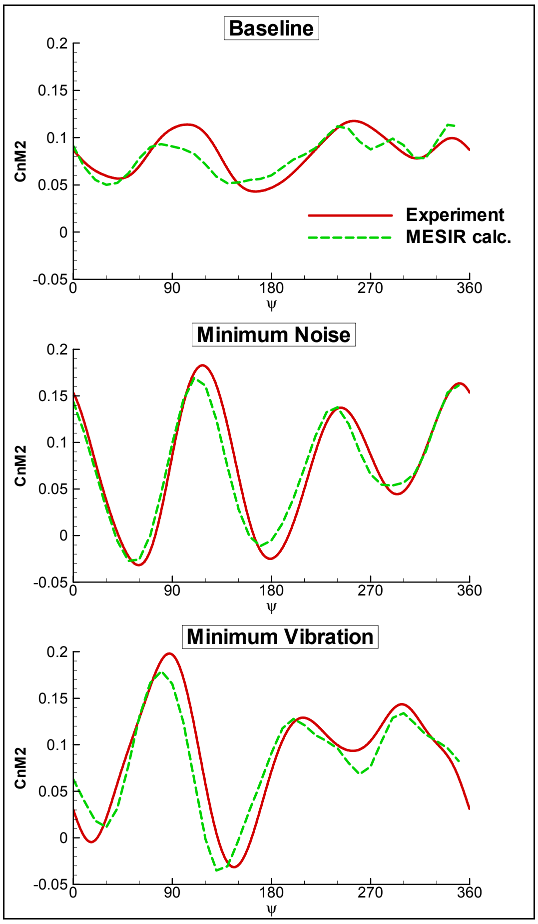

Figure 3: Sectional loads at r/R=0.87, low-pass filtered (up to 8/rev).

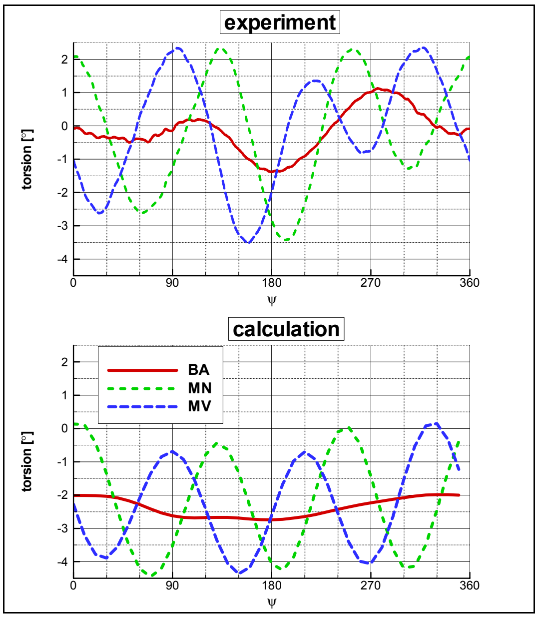

Figure 4: Experimental (top) and predicted (bottom) torsion deformations at the blade tip.

Wake geometry

In the previous paragraphs, it has been shown that the low frequency airloads were correctly predicted. This means that the strength of the vortices emitted by the blades should be well computed. This is a necessary but not sufficient condition for a good estimation of BVI noise. In particular, it is essential to check that the wake geometry (especially the position of the vortices with respect to the blades) are well predicted. Thanks to a visualisation technique called LLS [8], some limited wake data have been obtained during the HART tests, for a blade azimuth ψ=35°, just before the noisy blade-vortex interactions occur. In Figure 5, these measurements are compared with the MESIR vortex lattices which correspond to the tip vortex. More precisely, the side views of the LLS measurements have been used, since they contain most of the information to explain the influence of HHC on BVI noise (mainly the blade-vortex vertical distance), as shown in previous studies [9], [10]. In the Baseline case (Figure 5, top), the measured and predicted vortices pass very close to the blade (slightly below at the blade tip), and these interactions are almost parallel in the vertical plane: the agreement between the predicted vortices and the measurements is very good in this case. In the MN case (Figure 5, middle), the vortices pass much below the blades and the interactions are no longer parallel in the vertical plane: these two effects explain the BVI noise reduction. Note that the predicted vortices are located lower from the blades (approximately 250mm, which represents 2 chord lengths) as compared to experiment (150mm, more than 1 chord length). In the MV case, the vortices are located slightly over the blade, both in experiment and in the calculations. In this case, as mentioned in previous studies [9], [10], a complex vortex system made of pairs of counter-rotating vortices (because of the negative loading at the azimuths of emission), creates multiple blade-vortex interactions. Note that only the tip vortex (the one related to negative loading) has been represented in Figure 5 (bottom), even if the inboard vortex (predicted by the MESIR/MENTHE codes) has been found to be responsible for most of the BVI noise. However, this proves that the influence of HHC on the vortex geometry (and especially on the vortex convection in the vertical direction) is well captured by the computational method.

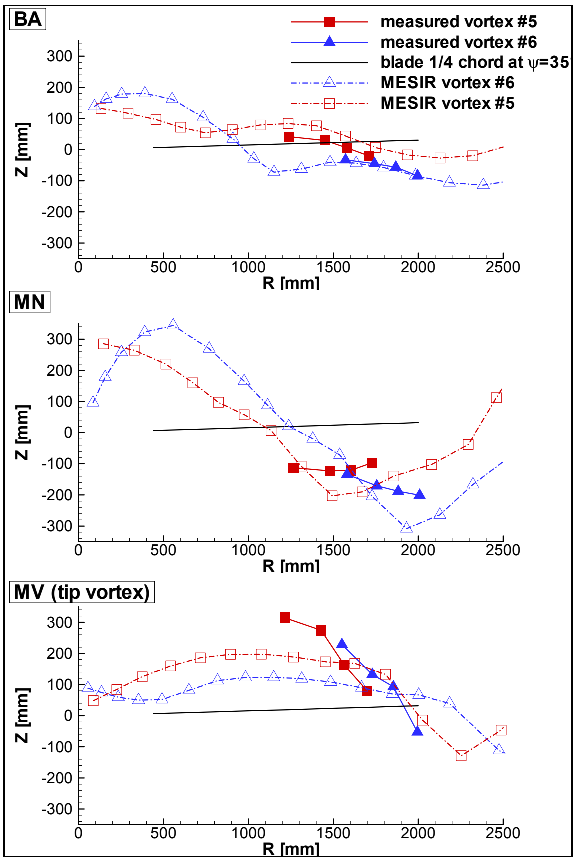

Figure 5: Measured (by LLS) and predicted tip vortex wake geometries. Side views representing the blade-vortex vertical miss-distances before interaction (ψ=35°)

Azimuthal derivatives of airloads

The best way to judge the accuracy of the BVI prediction before to run an acoustic calculation is to plot the azimuthal derivatives of the airloads histories, in order to see if the impulsive pressure fluctuations created by the blade-vortex interactions are correctly captured. As a matter of fact, the radiated noise is a direct function of the time derivatives of the pressure coefficients on the blades. The azimuthal derivatives of the CnM2 coefficients computed by the aerodynamic code ARHIS (which performs a calculation with a sufficiently small azimuthal step) are compared with the measurements in Figure 6, on the advancing side of the rotor disk (where the most impulsive blade-vortex interactions occur). The amplitude and phase of the peaks appearing on the d(CnM2)/dψ coefficients are generally fairly well predicted. In particular the following trends are captured:

- the absence of peaks in the MN case for ψ<70°, contrary to what happens on the Baseline case: this is responsible for the noise reduction in the MN case compared to the Baseline, and this is a direct consequence of the large blade-vortex distances mentioned in the previous paragraph,
- the multiplicity of peaks of large amplitude in the MV case.

Note that the very impulsive peak on the MN for ψ≈80° in the experiment (which does not generate significant noise because it is not a parallel interaction) is not predicted, as a consequence of the position of the vortices located too much below the blade in this case, as explained previously.

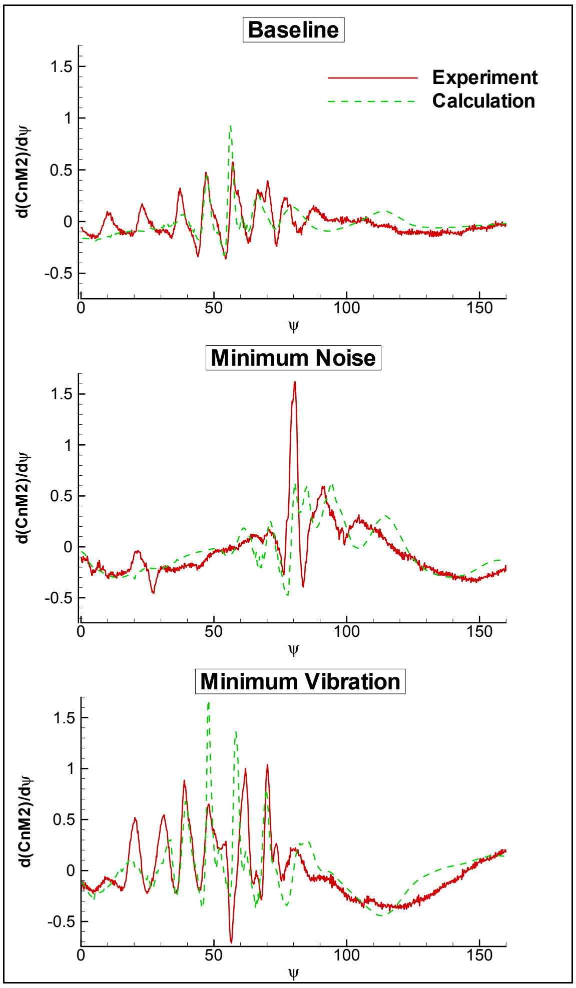

Figure 6: Azimuthal derivatives of sectional loads at r/R=0.87

<u>Noise contour levels</u>

A final validation of the computational chain is made on the noise contour levels in Figure 7. The agreement between calculations and experiment can be considered as quite good. In particular, the noise reduction in the MN case and, on the contrary, the noise increase in the MV case are correctly calculated. When looking into more details, it can be noticed that the noise reduction on the advancing side of the rotor disk is more pronounced in the calculations than in the measurements, probably due to the fact that the predicted vortices are too far from the blade (in the vertical direction) compared to the measured vortices, as shown previously.

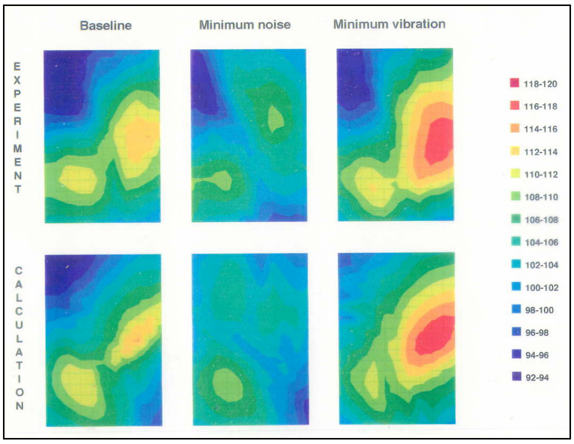

Figure 7: Noise contour levels. Experiment (top) and calculations (bottom)

Validation on 7AD/ERATO rotors

The ERATO program [11], [12], [13], launched in 1992, is a cooperation between ONERA, DLR and Eurocopter, aimed at designing and testing an aero-acoustically optimised rotor model, without penalties in terms of consumed power and dynamic loads. This program ended in 1998, with a proof of the design by means of wind-tunnel tests in the DNW and S1MA wind-tunnels [12]. The reference rotor for this program was the 7AD rotor, and the final ERATO optimised rotor had a very specific planform, with a double sweep concept (forward/backward), as illustrated by Figure 8.

<u>Test conditions</u>

One of the parameters that was part of the optimisation carried out in the ERATO program was the tip rotational Mach number M_{tip}. The reference M_{tip} for the 7AD rotor was equal to 0.661, whereas the studies led to the conclusion that a reduced M_{tip} equal to 0.617 would be beneficial for the ERATO rotor. The reference value M_{tip}^*=0.617 has been used in the comparisons between the two rotors to define typical reference advance ratio μ*=0.165 and nominal thrust coefficient Zb_w*=12.5 (the subscript w is here related to the assumed weight of the helicopter). This means that the comparisons are always made for the same physical advancing velocity V_0 and rotor thrust, whatever the tip rotational Mach number is. In the following parts, test conditions with different descent angles α_d ranging from –2° to –10° are considered.

The prediction results presented below have been obtained accounting for the elastic deformations of the blades.

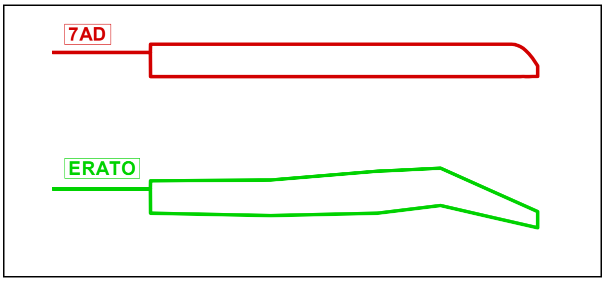

Figure 8: 7AD and ERATO blades planform

<u>Comparison between calculations and experiment at 6° descent angle</u>

Examples of comparison of sectional loads (low-pass filtered, up to 8/rev) between calculations and experiment are presented in Figure 9 for the 7AD rotor and in Figure 10 for the ERATO rotor. The CnM2 time histories for the 7AD rotor are well predicted and the spanwise evolution of sectional loads for ψ=140° are also in good agreement with experiment. For the ERATO rotor, the computations underpredict the 4/rev component of the CnM2 azimuthal histories (Figure 10, left): this is due to a poor prediction of the dynamic behaviour of the ERATO rotor, especially the tip torsion history. Fortunately, this seems to have a limited influence on the spanwise evolution of CnM2 for ψ=140°, which is fairly well predicted (Figure 10, right). Looking into more details at the CnM2 for ψ=140° for the two rotors (Figure 9 and Figure 10, right), one notices that the gradient of CnM2 radial evolution is much more pronounced on the 7AD rotor than on the ERATO rotor, so that the strength of the vortices emitted by the ERATO rotor in the second quadrant should be reduced compared to the vortices emitted by the 7AD rotor. This is consistent with the analysis of PIV data (Figure 11 taken from [12]), which clearly indicates reduced intensity for the main vortices of the ERATO rotor compared to the 7AD rotor. This was expected from the optimisation and this is one of the reasons for the noise reduction observed on the ERATO rotor. Furthermore, one can notice that the airloads are slightly negative at the tip of the 7AD rotor (Figure 9, right), which leads to the prediction of two vortices: one tip vortex with a small negative (non conventional) intensity, and a main vortex of positive intensity (responsible for noise), which is the most intense one, and is emitted more inboard. To some extent, this vortex structure is comparable to what has been observed on the Bo105 rotor for the MV case of the HART database, but in the present case, this is obtained by passive means (shape of the 7AD blade tip) instead of active means (HHC).

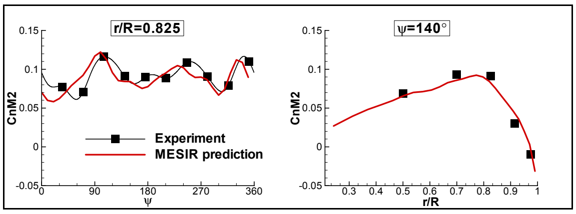

Figure 9: Sectional loads for the 7AD rotor, low-pass filtered (up to 8/rev): M_{tip}=0.661, Zb_w=12.5, α_d=-6°*

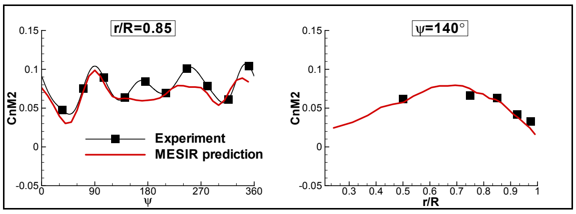

Figure 10: Sectional loads for the ERATO rotor, low-pass filtered (up to 8/rev): M_{tip}=0.617, Zb_w=12.5, α_d=-6°*

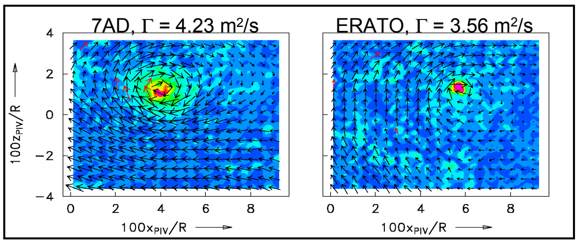

Figure 11: PIV plots of main vortices emitted by the 7AD and ERATO rotors and resulting vortex intensities

For some limited test conditions, the wake geometry of the 7AD and ERATO rotors has been measured using the same LLS technique as in the HART program. For the 7AD rotor, the predicted wake geometry for an azimuth angle ψ=45° is in good agreement with experiment, not only in the top view (Figure 12, top), but also in the side view (Figure 12, bottom): note that the four represented vortex lattices interact with the blade within a vertical distance of the order of +/- half a chord length (1 chord length=140mm). However, it can be seen that the predicted vortices are located slightly too much downwards (approximately 20% chord length in the vertical direction), as compared to the measurements. For the ERATO rotor, the agreement with experiment remains quite good on the top view (Figure 13, top), but it is rather poor in the side view (Figure 13, bottom), where the vertical distance between two consecutive vortices is by far too large in the predictions compared to experiment.

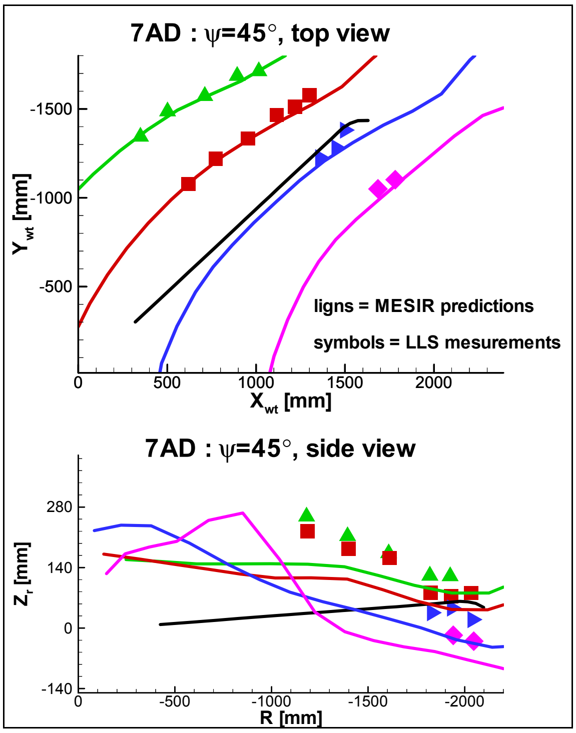

Figure 12: Wake geometry for the 7AD rotor (M_{tip}=0.617, Zb_w=12.5, α_d=-6°). Inboard vortex represented.*

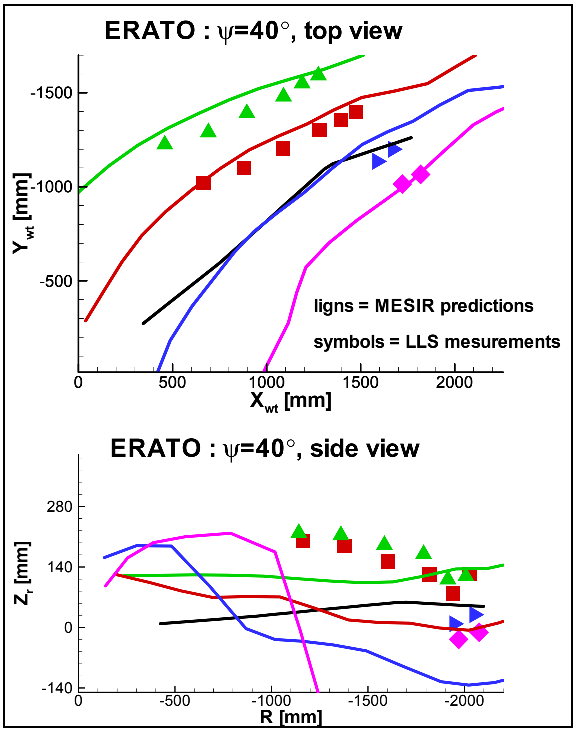

Figure 13: Wake geometry for the ERATO rotor (M_{tip}=0.617, Zb_w=12.5, α_d=-6°).*

Despite the poor agreement of the wake geometry of the ERATO rotor, the computational chain succeeds in predicting the noise reduction obtained for α_d=-6° with the ERATO rotor, as illustrated in Figure 14. However, one can notice an overestimation of the gains obtained with the ERATO rotor by comparison with the reference 7AD rotor. In fact, the predicted noise difference is about 6.4dBA (mean level) and it was measured 3.7dBA in the experiment. One part of these differences is due to the reduced tip rotational Mach number on the ERATO rotor.

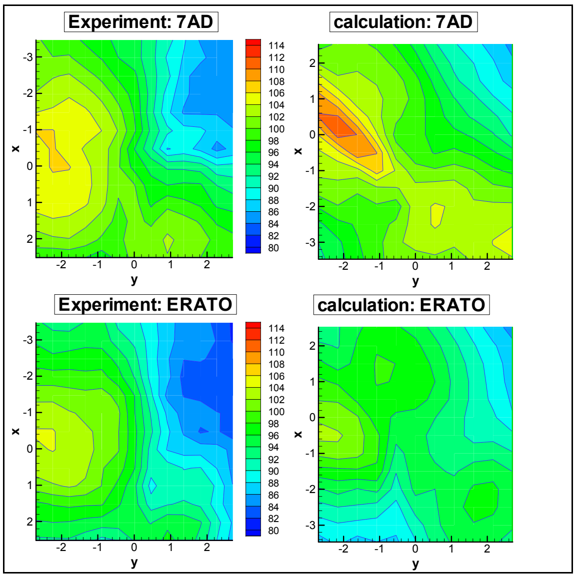

Figure 14: Noise contour levels (Zb_w=12.5, α_d=-6°). 7AD: M_{tip}=0.661, ERATO: M_{tip}=0.617*

Sweep in descent angle

For a passive rotor blade optimisation, it is very important to check that the gains observed for a given flight condition are also valid for a wide range of flight conditions. In the case of acoustic optimisation, special attention has to be paid to the influence of descent angle, since a real helicopter never flies on a pure –6° path slope (in reality some deviations of +/-2° are often encountered). The measurements done in the DNW have shown noise reductions for descent angles ranging from –2° up to –8°, with a maximum gain for α_d=–4° (Figure 15, left). Even if the predictions are more optimistic (Figure 15, right), the computational chain succeeds in predicting the relative mean noise levels between the 7AD and ERATO rotors.

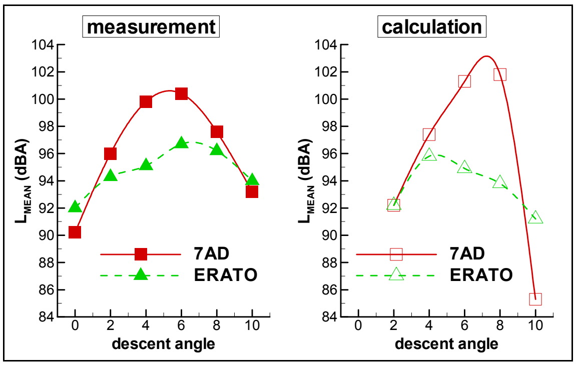

Figure 15: Mean noise levels (Zb_w=12.5): measured (left) and computed (right). 7AD (M_{tip}=0.661) and ERATO (M_{tip}=0.617)*

This relatively good result can be surprising, considering the poor prediction of the wake geometry of the ERATO rotor (in the side view) mentioned previously. In fact, a deeper analysis of the results has shown that the three main reasons for the noise reduction with the ERATO blade design are:

- the reduced vortex intensity (which is correctly predicted),
- the non parallel interactions between the ERATO blade and the vortices in the horizontal plane, due to the forward/backward sweep concept (which is by definition accounted for in the calculations),
- the reduced tip Mach number on the ERATO rotor, the influence of which is correctly evaluated.

<u>Influence of blade elasticity on blade shape optimisation</u>

The predictions presented before have been done using all the aero-elastic blade degrees of freedom. However, during the design phase of the ERATO blade, most of the parametric studies were done assuming rigid blades. In this part, the influence of blade elasticity is studied in order to quantify its influence on the radiated noise levels. This study is done for a lift coefficient Zb_w*=17.5 (higher than the nominal lift coefficient equal to 12.5), because it is the case for which the relative differences between the two rotors were the most pronounced.

The influence of the elastic deformations of the blades on the spanwise evolution of the sectional loads CnM2 is rather small for both rotors (Figure 16), because the torsion deformations are not very large, especially on the advancing side (Figure 17), contrary to what has been noticed on the Bo105 rotor. Consequently, the wake geometry is not significantly modified and the maximum noise levels are modified by approximately 1dBA (depending on the descent angle: Figure 18). The relative noise differences between the 7AD and ERATO rotors remain globally the same.

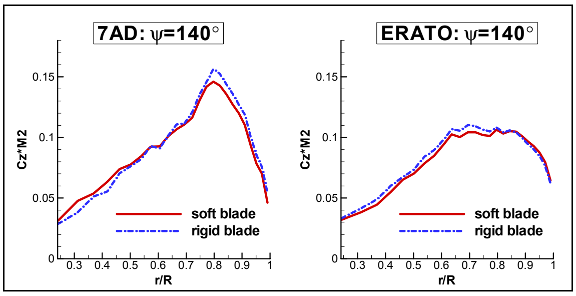

Figure 16: Influence of elasticity on CnM2 (Zb_w=17.5, α_d=-6°).*

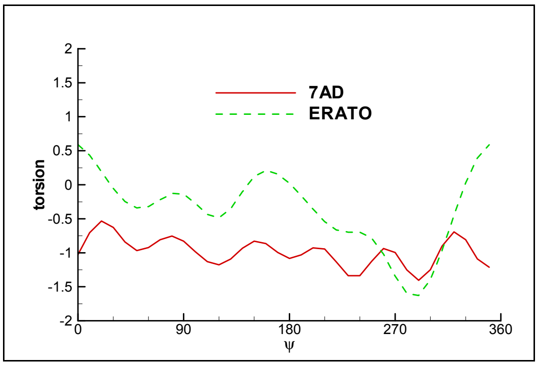

Figure 17: Torsion deformations (r/R=1, Zb_w=17.5, α_d=-6°).*

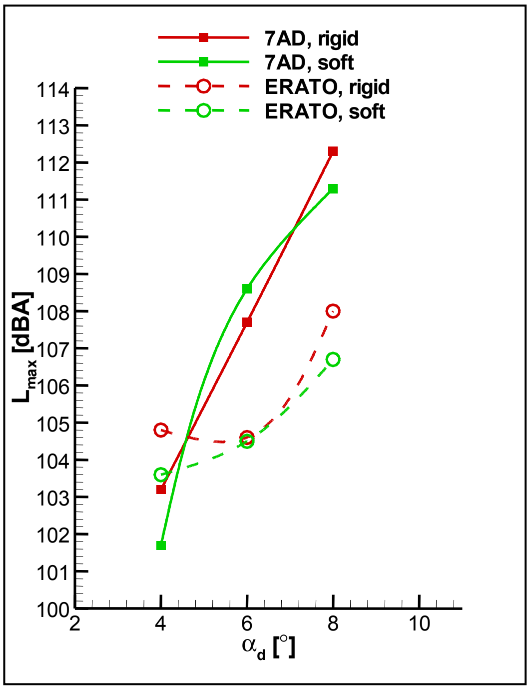

Figure 18: Influence of elasticity on maximum predicted noise levels (Zb_w=17.5, α_d=-6°).*

Influence of trim procedure in the calculation

As mentioned in the codes description, the blade motion is an input of the free wake analysis, which means that the wake distortion is assumed to have no significant influence on the rotor trim. To check this, an iterative coupling has been made between the HOST code and the MESIR code as follows: the wake geometry at the end of a MESIR calculation is used in a new rotor trim analysis made by HOST. This new rotor trim is then used as an input for a new free wake analysis. This iterative procedure is done until convergence, which is achieved when the control angles (pitch, flapping) and blade deformations remain unchanged between two consecutive iterations. The coupling process converges quite fast, since only three iterations are necessary. Of course, this means three free wake calculations, so that the CPU time increases dramatically. Figure 19 shows that this procedure has a very limited effect on the radiated noise prediction: the difference between the conventional computation without coupling (left) and with coupling (right) differs by only 0.6 dBA for the 7AD rotor (top of Figure 19) or for the ERATO rotor (bottom of Figure 19), which is negligible. This shows that, at least in the test cases considered here, the rotor trim procedure is not significantly affected

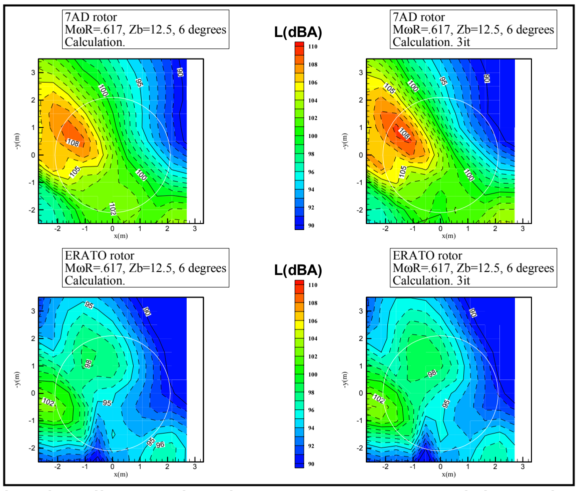

by the distorted wake geometry, as anticipated.

Figure 19: Influence of iterative coupling between the rotor trim and wake geometry on noise contour levels (left: no coupling, right: with coupling, top: 7AD, right: ERATO)

Application to blades with flaps

A promising way to reduce the noise generated by the main rotor blades is the use of active concepts, such as active trailing-edge flaps. In this case, contrary to the passive optimisation done in the ERATO program, the noise can be reduced actively, which means that, for each particular flight condition, the flap deflection azimuthal history can be optimised.

Within the French-German Active Blade Concept (ABC) program [14], ONERA and DLR have the objective to design and test in the S1MA and DNW wind-tunnels a 4-bladed rotor model equipped with trailing-edge flaps (Figure 20). Typical results of the aero-acoustic investigations are presented below. Since the wind-tunnel tests are planned in 2004 and 2005, no comparison with experiment is presented.

Specific codes adaptations

Only limited adaptations of the ONERA computational chain presented before have been necessary to compute blades with trailing-edge flaps. In the two first steps of the predictions (HOST and MESIR codes), the influence of the flap is taken into account through 2D look-up tables, generated for different flap deflections: δ_f=-5°, 0°, +5°, +10° (δ_f positive for the flap deflected downwards).

Consequently, in addition to the interpolation of Mach number and incidence, an additional interpolation of the flap angle deflection is done, assuming a linear evolution of the aerodynamic coefficients with respect to the parameter δ_f.

The roll-up model (MENTHE) is able to take into account with no modification the vortical structures that can be generated by a flap: in addition to the conventional blade tip vortex, an inboard flap vortex and an outboard flap vortex can be generated and are automatically detected.

Blade geometry

The ABC blade shape that has been chosen for wind-tunnel tests is represented in Figure 20: it is equipped with a trailing-edge flap of 0.10R span extension (located between r/R=0.8 and 0.9) and 15% chord depth (this geometry being a result of the investigations carried out in the ABC project and taking into account the constraints provided by industry).

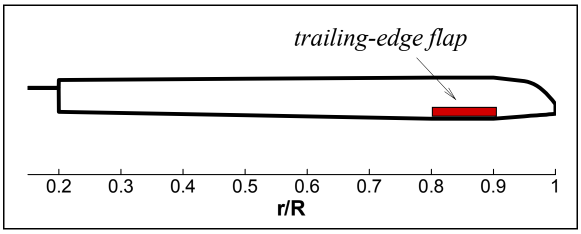

Figure 20: Geometry of the ABC blade with trailing-edge flap between r/R=0.8 and 0.9

Two different structural definitions of this blade are investigated in the present paper: the first one (ABC-Mod12 blade) yields to a torsion frequency equal to 5.3/rev, and the second one (ABC-Mod11 blade) yields to a torsion frequency equal to 4.6/rev. This means that the second design is softer in torsion than the first one. Investigations of the efficiency of different flap deflection laws for these two designs are presented below.

Noise reduction through wake convection

As demonstrated by the HART programs, a very efficient way to reduce BVI noise is to modify (increase) the blade-vortex vertical miss-distance. To achieve this, it is necessary either to increase (for a convection downwards) or to decrease (for a convection upwards) the airloads (and so the induced velocities) on the trajectory of the vortices. Practically, this can be achieved by twisting the blade, by means of HHC in the case of the HART Bo105 rotor, and possibly with an active trailing-edge flap in the ABC project. Indeed, a flap actuation can modify the blade torsion response since a flap deflected downwards (δ_f positive) creates a negative (nose down) aerodynamic pitching moment. If the phase and the frequency of the flap actuation are well chosen, this is likely to create torsion elastic deformations.

For the ABC blades, parametric studies have shown that a 4/rev actuation was the most effective to create a torsion response. More precisely, a 4/rev flap deflection with an amplitude of 5° (half peak-to-peak) can generate significant torsion deformations for the ABC-Mod11 blade (more than 4° peak-to-peak), but generates only a 2° peak-to-peak torsion response for the ABC-Mod12 blade, which is not enough to expect significant modifications of the convection of the vortices.

To quantify the potential acoustic gains on the ABC-Mod11 blade design, two different flap deflection laws, called 4ΩH and 4ΩB (plotted in Figure 21) have been tested: the first one (4ΩH) creates negative (nose down) pitching moments on the advancing side of the rotor disk and consequently reduces the airloads in this area by more negative torsion deformations (Figure 22), whereas the other flap deflection law (4ΩB) has exactly the opposite effect. Compared to the reference condition without any flap deflection, the 4ΩH law creates an upwash on the vortex trajectories and the 4ΩB law creates a more pronounced downwash (Figure 23).

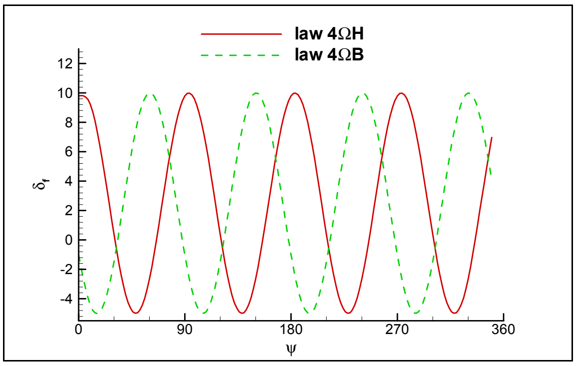

Figure 21: Flap deflections laws 4ΩB and 4ΩH

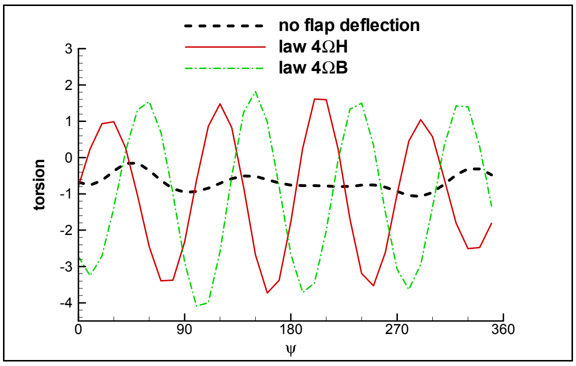

Figure 22: Torsion response of blade ABC-Mod11 with the 4ΩB and 4ΩH flap deflection laws

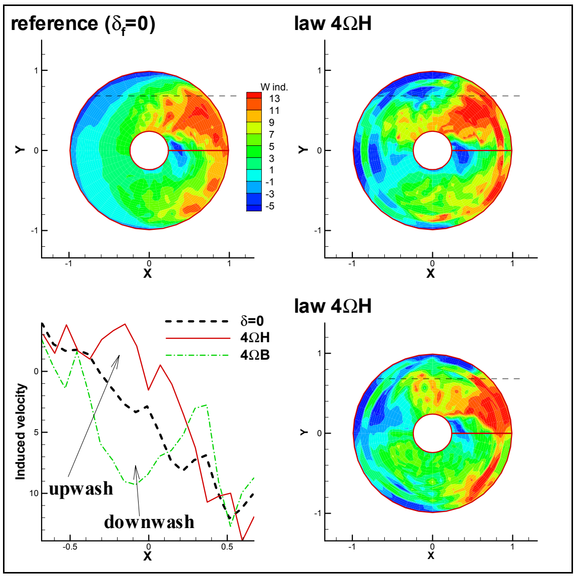

Figure 23: Influence of flap deflection law on Induced velocities

The blade-vortex miss-distances are increased in both cases (in the upwards direction with the 4ΩH law and downwards with the 4ΩB law). In both cases, this leads to significant noise reductions (of the order of 5dBA), as illustrated by Figure 24 for a 8° descending flight condition.

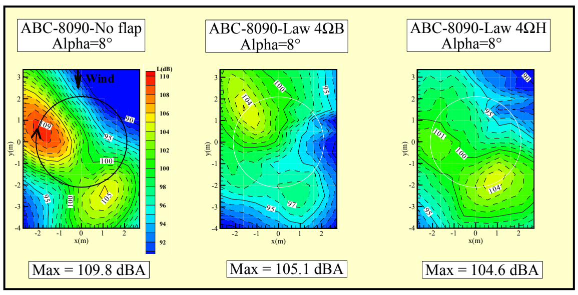

Figure 24: Influence of flap deflection law on noise levels

Noise reduction through vortex arrangements

In the case of the ABC-Mod12 rotor design, the pitching moment created by a flap deflection of reasonable amplitude (+/- 5°) is not sufficient to create a torsion excitation, because the blade is too stiff in torsion. In this case, another strategy to reduce the BVI noise may be proposed: it consists in a flap deflection law (called Law3mod hereafter) such that the flap is deflected slightly upwards (δ_f<0) at the azimuth angles where the vortices are emitted. By doing this, there is a possibility to create two co-rotating vortices (one flap outboard vortex and one blade tip vortex), as illustrated in Figure 25.

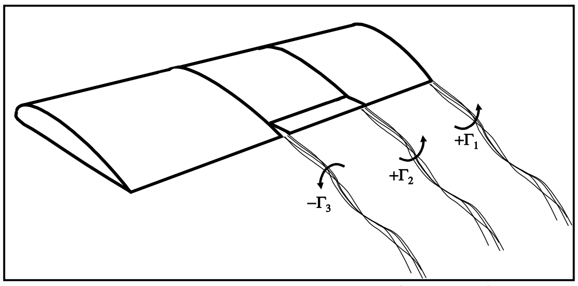

Figure 25: Two co-rotating vortices ($+\Gamma_1$, $+\Gamma_2$) with a flap deflected upwards

This particular vortex arrangement can reduce the impulsivity of the pressure fluctuations when the vortices interact with the blade, in a way similar to what was obtained with the “vane tip” concept [15]. The noise reduction using this kind of flap deflection is not as high as the one obtained by modifying the vortex convection, but it can reach 4 dBA (Figure 26), according to the predictions. It has to be noted that the result of the prediction strongly depends of the validity of the criteria used in the roll-up model code MENTHE to detect the generation of co-rotating vortices. These criteria will be validated only after the wind-tunnel tests.

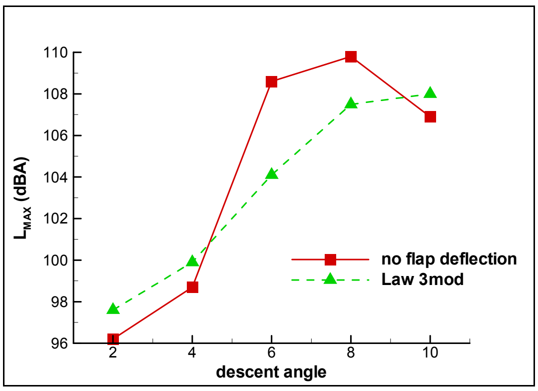

Figure 26: Maximum noise levels without and with flap deflection (Law3mod)

Conclusions

The ONERA method for the prediction of BVI noise has been presented and validated by comparison with two databases obtained in wind-tunnel within the HART and ERATO programs. This validation has been made step-by-step, with detailed analysis of the results at each step of the five methods of the computational chain.

On the HART database (Bo105 rotor), it has been shown that the influence of HHC on sectional loads, torsion deformations, wake geometry and radiated noise is fairly well predicted. A deeper validation of the wake geometry will be done in a near future, using the 3C-PIV data obtained within the HART II program.

The same computational method has been used to design the ERATO aero-acoustically optimised rotor, equipped with non conventional blades characterised by a double sweep concept. The calculations succeed in predicting the relative differences between the optimised ERATO rotor and the reference 7AD rotor, although the wake geometry generated by the complex planform of the ERATO blade is not well captured.

Finally, thanks to the computational tools, two strategies to reduce the BVI noise by the use of trailing-edge flaps have been proposed: a validation of this study will be done once the ABC wind-tunnel model rotor tests are completed (2004-2005).

Improvements of the key part of the present computational chain (free wake model) have already been undertaken. They concern the development of a new free wake model able to account for non conventional blade planforms through the use of the curved lifting-line theory (closer to a lifting-surface model), able to simulate unsteady flight manoeuvres. In the long term, one can expect to use directly the Computational Fluids Dynamics methods (Euler or Navier-Stokes) to capture the blade-vortex interactions and compute the BVI noise, which will be very attractive, since these methods do not necessitate a wake model as the singularity methods.

Acknowledgements

The authors would like to acknowledge the DGA and the DGAC for their financial support on the HART, ERATO and ABC projects.

References

[1] Toulmay, F., Arnaud, G., Falchero, D., Villat, V.: *Analytical Prediction of the Rotor Dynamics for Advanced Geometry Blades*, 52nd Annual Forum of the American Helicopter Society, Washington DC, June 1996

[2] Benoit, B., Dequin, A.-M., Kampa, K., Grunhagen, W., Basset, P-M., Gimonet, B.: *HOST, A General Helicopter Simulation Tool for Germany and France*, 56th Annual Forum of the American Helicopter Society, Virginia Beach, May 2000

[3] Michéa, B., Desopper, A., Costes, M.: *Aerodynamic Rotor Loads Prediction Method with Free Wake for Low Speed Descent Flight*, 18th European Rotorcraft Forum, Avignon, September 1992

[4] Rahier, G., Delrieux, Y.: *Improvement of Helicopter Rotor Blade-Vortex Interaction Noise Prediction using a Rotor Wake Roll-Up Model*, 16th AIAA Aeroacoustic Conference, München, June 1995

[5] Spiegel, P., Rahier, G., Michéa, B.: *Blade-Vortex Interaction Noise: Prediction and Comparison with Flight and Wind Tunnel Tests*, 18th European Rotorcraft Forum, Avignon, September 1992

[6] Spiegel, P., Rahier, G.: *Theoretical Study and Prediction of BVI Noise Including Close Interactions*, AHS Technical Specialists Meeting on Rotorcraft Acoustics and Fluids Mechanics, Philadelphia, PA, October 1991

[7] Spiegel, P.: *An Iso-Event Spanwise Interpolation Technique for Blade-Vortex Interaction Noise Prediction and Analysis*, 24th European Rotorcraft Forum, Marseille, September 1998

[8] Kube, R., Splettstoesser, W., Wagner, W., Seelhorst, U., Yu, Y., Boutier, A., Micheli, F., Mercker, E.: *Initial Results from the Higher Harmonic Control Aeroacoustic Rotor Test (HART) in the German-Dutch Wind-Tunnel*, 75th AGARD Fluid Dynamic Panel Meeting on Aerodynamics and

Aeroacoustics of Rotorcraft, Berlin, October 1994

[9] Beaumier, P., Spiegel, P.: *Validation of ONERA aeroacoustic prediction methods for Blade-Vortex Interaction Using HART tests results*, 51st Annual Forum and Technology Display, AHS, Fort Worth, May 1995

[10] Van der Wall, B.: *Vortex Characteristics Analysed from HART Data*, 23rd European Rotorcraft Forum, Dresden, 1997

[11] Prieur, P., Splettstoesser, W.: *ERATO – an ONERA-DLR Cooperative Programme on Aeroacoustic Rotor Optimisation*, 25th European Rotorcraft Forum, Roma, September 1999

[12] Splettstoesser, W., Van der Wall, B., Junker, B., Schultz, K., Beaumier, P., Delrieux, Y., Leconte, P., Crozier, P.: *Wind Tunnel Test Results and Proof of Design for an Aeroacoustically Optimized Rotor*, 25th European Rotorcraft Forum, Roma, September 1999

[13] Delrieux, Y., Prieur, J., Costes, M., Gardarein, P., Beaumier, P., Mercier des Rochettes, H., Leconte, P., Crozier, P., Splettstoesser, W.R., van der Wall, B., Junker, B., Schultz, K.-J., Mercker, E., Pengel, K., Philippe, J-J., Gmelin B.: *The Onera-DLR Aeroacoustic Rotor Optimisation Programme ERATO: Methodology and Achievements*, AHS-Aerodynamics, Acoustics, and Test and Evaluation Technical Specialists Meeting, San Francisco, January 2002

[14] Leconte, P., Rapin, M., Van der Wall, B.: *Main Rotor Active Flaps: Numerical Assessment of Vibration Reduction*, 57th Annual Forum of the AHS, Washington DC, May 2001

[15] Brocklehurst, A., Pike, A.C.: *Reduction of BVI using a Vane Tip*, AHS Aeromechanics Specialists Conference, San Francisco, January 1994